# Stable Hopf-Skyrme topological excitations in the superconducting state

Filipp N. Rybakov,[1] Julien Garaud,[2] and Egor Babaev[1,*]
[1]*Department of Physics, KTH-Royal Institute of Technology, Stockholm, SE-10691 Sweden*
[2]*Institut Denis-Poisson CNRS/UMR 7013, Université de Tours-Université d'Orléans, Parc de Grandmont, 37200 Tours, France*

(Received 18 September 2018; revised manuscript received 22 January 2019; published 10 September 2019)

At large scales, magnetostatics of superconductors is described by a massive vector field theory: the London model. The magnetic field cannot penetrate into the bulk unless quantum vortices are formed. These are topological excitations characterized by an invariant: the phase winding. The London model dictates that loops of such vortices are not stable because the kinetic energy of superflow and the magnetic energy are smaller, the smaller vortex loops are. We demonstrate that in two-component superconductors, under certain conditions, such as the proximity to pair-density-wave instabilities, the hydromagnetostatics of the superconducting state and topological excitation changes dramatically: the excitations acquire the form of stable vortex loops and knots characterized by the different topological invariant: the Hopf index and hence termed hopfions. This demonstrates that magnetic properties in a superconducting state can be dramatically different from those of a London's massive vector field theory.

DOI: 10.1103/PhysRevB.100.094515

## I. INTRODUCTION

The basic macroscopic excitations produced by fluctuations and quenches in an ordinary superconducting state are closed or knotted vortex loops. Once formed, these loops are unstable and decay. The question of the existence of stable knotted vortices was raised by Kelvin in the context of the "vortex-atoms" theory, which identified atoms to knotted vortices in luminiferous aether [1]. This theory was falsified after Michelson and Morley's experiment ruled out the existence of aether. Yet, this attempt to build a periodic table of chemical elements as topologically distinct vortex knots, and interpret matter as their bound states, had a profound impact on both mathematics and physics. The necessity to classify different knots topology in this theory has initiated the field of knot theory in mathematics [2]. In physics, the principle to associate topological defects of an underlying field with "particles," forming "matter," reemerged on multiple occasions, notably in Skyrme's work, which aimed at describing nucleons as topological solitons [3].

Different particle-vortex dualities were eventually well established in modern condensed matter physics, most notably in theories of superfluids and superconductors. The basis for the duality involves three paradigm-shifting concepts introduced in Onsager's work on superfluids [4]. First was the observation that superfluid velocity circulation is quantized, and thus that vortices carry a quantized topological charge. The second observation was that the rotation of a superfluid results in the formation of a lattice or a liquid of quantum vortices, i.e., vortex-lines realization of crystals and liquids. The third crucial concept is that vortex matter controls many of the key responses of superfluids. For example, the superfluid to normal state phase transition is a thermal generation and proliferation of vortex loops and knots [4]. Subsequently, this was put on firm theoretical grounds by Feynman [5]. The superconducting phase transition was likewise demonstrated to be driven by the proliferation of vortex loops [6]. A remarkable particle-vortex duality that describes macroscopic responses of a system can also be found in the Berezinskii, Kosterlitz, and Thouless theory [7,8] of two-dimensional superfluids, where vortices with opposite circulations are mapped onto particles and antiparticles. In three dimensions, thermal and quench responses, and turbulent states, are collective states of vortex loops and knots. However, the crucial difference from the objects that were conjectured in Kelvin's theory is that vortex loops and knots are intrinsically unstable, as follows from Derrick's theorem [9]. This implies that an excited system forms vortex loops and knots that tend to collapse, as the kinetic energy of the superflow always decreases for smaller loops or knots. This instability is physically important as it dictates many of the universal hydrodynamics-based macroscopic properties of presently known superfluids and superconductors.

Knotted field configurations have been recently found and investigated in a broad variety of different physical systems [10–15]. Research on models supporting stable knots has been of great interest after stability of these objects, characterized by a Hopf topological invariant, was found in the so-called Skyrme-Faddeev model, which opened new research directions in mathematical physics [16–20]. This is a model for a three-component unit vector $\vec{n} = (n_1, n_2, n_3)$, with energy density, $\mathcal{E}_{\rm SF} \propto (\nabla \vec{n})^2 + (\vec{n} \cdot \partial_i \vec{n} \times \partial_j \vec{n})^2$. While seemingly unrelated to superconductivity, it was observed that there exists a formal relation with Ginzburg-Landau theories of multicomponent superconductors [21,22]. Namely, two-component Ginzburg-Landau models can be mapped onto a Skyrme-Faddeev model coupled to an additional massive vector field. This observation motivated the conjecture that multicomponent superconductors may support stable knots with nontrivial Hopf invariant, also termed in various contexts

*babaev@kth.se

 

knotted solitons, knot solitons, and hopfions. Detailed numerical studies, however, have not demonstrated stability [23]. Reasons for such instability include that the magnetostatic properties are still well approximated by the London model as was subsequently discussed both using physical estimates [24] and formal mathematical approaches [25]. Despite different analytical arguments made in favor of (meta)stability [24,26] and findings of the stability of knots in mathematical generalizations of the Skyrme-Faddeev model coupled to gauge fields [25,27,28], the prevalent opinion today is that, similarly to superfluids, knotted vortices are unstable in superconductors.

We demonstrate here that in a class two-component superconducting states, knotted vortices are stable. Many of the superconducting states of recent interest are characterized by multicomponent order parameters. This occurs for various reasons such as chiral or nematic states (for recent examples see, e.g., [29,30]), or for example due to coexistence of the superconductivity of electrons and nucleons [31–35]. A generic, but often neglected, effect in multicomponent superconductors and superfluids is current-current interaction, also known as the Andreev-Bashkin effect [36,37]. Namely, in superfluid mixtures with two components, due to the intercomponent interactions occurring between particles, the current of a given component $\boldsymbol{j}_{1,2}$ generically depends on the superfluid velocities $\boldsymbol{v}_{1,2}$ of both as follows:

$$\boldsymbol{j}_1 = \rho_{11}\boldsymbol{v}_1 + \rho_{12}\boldsymbol{v}_2 \quad \text{and} \quad \boldsymbol{j}_2 = \rho_{22}\boldsymbol{v}_2 + \rho_{21}\boldsymbol{v}_1. \tag{1}$$

Here, the coefficients $\rho_{12}$ and $\rho_{21}$ determine the fraction of the density of one of the superfluid components carried by the superfluid velocity of the other: i.e., the intercomponent drag. Drag coefficients $\rho_{12}$ and $\rho_{21}$ can be very large, for example, in spin-triplet superconductors and superfluids [38], Fermi-liquid mixtures [31,32], or strongly correlated systems [39–41].

## II. MODEL

Two-component superconductors are described by a doublet $\Psi = (\psi_1, \psi_2)^{\mathrm{T}}$ of complex fields $\psi_a = |\psi_a| e^{i\varphi_a}$ (with $a = 1, 2$), whose squared moduli $|\psi_a|^2$ represent the density of individual superconducting components. Each of the components is coupled to the vector potential $\boldsymbol{A}$ of the magnetic field $\boldsymbol{B} = \nabla \times \boldsymbol{A}$, via the gauge derivative $\boldsymbol{D} = \nabla + ig\boldsymbol{A}$. Such a system is described by the Ginzburg-Landau free energy $E = \int \mathcal{E}\, d\mathbf{r}$, whose density reads as

$$\mathcal{E} = \frac{\boldsymbol{B}^2}{2} + \sum_{a=1,2} \frac{\gamma_a}{2} |\boldsymbol{D}\psi_a|^2 + \sum_{a,b=1,2} \frac{\mu_{ab}}{2} \boldsymbol{J}_a \cdot \boldsymbol{J}_b \tag{2a}$$

$$+ \nu(\Psi^\dagger \Psi - 1)^2 + V[\Psi, \Psi^\dagger], \tag{2b}$$

where $\boldsymbol{J}_a = \mathrm{Im}(\psi_a^* \boldsymbol{D}\psi_a) = |\psi_a|^2(\nabla\varphi_a + g\boldsymbol{A})$.

The terms $\mu_{12} = \mu_{21}$ of the current coupling matrix $\hat{\mu}$ describe the intercomponent drag [31,32,36,38–41]. The total current is the sum of supercurrents in individual components, which have a similar structure to that described in (1). The first term in (2b) is responsible for the condensation of superconducting electrons, such that in the ground state, $\Psi^\dagger\Psi \neq 0$. For ordinary type-II superconductors, a good approximation is the constant-density (London limit), here it is equivalent to $\nu \to \infty$ in (2b). In the simulations we considered the case of g = 1.

Many two-component superconducting states spontaneously break $\mathrm{U}(1)\times\mathrm{U}(1)$, $\mathrm{U}(1)\times\mathbb{Z}_2$, or U(1) symmetries (see, e.g., [29,30,33–35]). Corresponding symmetry-breaking potential terms are collected in $V[\Psi, \Psi^\dagger]$, whose structure is detailed in Appendix A. For a discussion of the relationship between the related, but less general, Ginzburg-Landau and Skyrme-Faddeev models see [24,42].

## III. TOPOLOGICAL CHARGE

In two-component superconductors, the simplest vortices feature $2\pi$ phase winding only in one of the components, e.g., when on a closed contour surrounding the vortex core is $\oint \nabla\varphi_1 \cdot d\boldsymbol{\ell} = 2\pi$ while $\oint \nabla\varphi_2 \cdot d\boldsymbol{\ell} = 0$. These are called fractional vortices (for further details, see, e.g., [37,43]). Integer flux carrying defects are composite of two fractional vortices. Topologically nontrivial knotted vortex loops consist of linked or knotted loops of fractional vortices in each component. As in Kelvin's picture, there are infinitely many ways to knot and link such objects. Topological considerations imply that knotted vortices are characterized by an integer topological index $\mathcal{Q}$ (see, e.g., discussions given in Refs. [11,16,18,21–24]). This index, which is conserved when fractional vortices of different components cannot cross one another, is defined as (see Appendix B)

$$\mathcal{Q} = -\frac{1}{12\pi^2} \int_{\mathbb{R}^3} \varepsilon_{ijk}\varepsilon_{abcd}\, \zeta_a \frac{\partial\zeta_b}{\partial r_i} \frac{\partial\zeta_c}{\partial r_j} \frac{\partial\zeta_d}{\partial r_k} d\mathbf{r}\,, \tag{3}$$

where $\boldsymbol{\zeta} = (\mathrm{Re}\,\psi_1, \mathrm{Im}\,\psi_1, \mathrm{Re}\,\psi_2, \mathrm{Im}\,\psi_2)/\sqrt{\Psi^\dagger\Psi}$, and where $\varepsilon$ is the Levi-Civita symbol. Index $\mathcal{Q}$ is always an integer unless $\Psi$ has zeros. The situation where $\Psi = 0$ can appear when cores of fractional vortices of different components intersect. However, in the case a constant density, this situation is impossible. Importantly, if this constraint is removed, we did not observe core intersections in numerical simulations for the considered regimes. Transient vortex states characterized by similar kind of topological indices are rather generic for two-component superfluids and were experimentally observed [15]. In superfluids, however, such vortex knots represent nonstationary objects which are unstable against shrinkage. The corresponding topological index vanishes when loops shrink without potential barriers, therefore knotted vortex configurations in this kinds of superfluids do not represent topological solitons analogous to discussed in [16–20].

## IV. RESULTS AND DISCUSSION

To investigate the existence of stable knotted vortices in two-component superconductors, we performed a numerical minimization of the free-energy functional (2), starting from various initial states of knotted and linked vortex loops. The numerical computations are related, in a way, to the relaxation processes of vortex tangles forming due to thermal fluctuations or quenching. Such three-dimensional optimization problems are highly computationally demanding, which we address with a code designed for graphic processing units (GPUs) (see Appendix A for details). Upon finding stable knotted solutions for various parameters of the model (2), an in-depth investigation of solutions for various values of the topological index $\mathcal{Q}$ was performed within the London limit

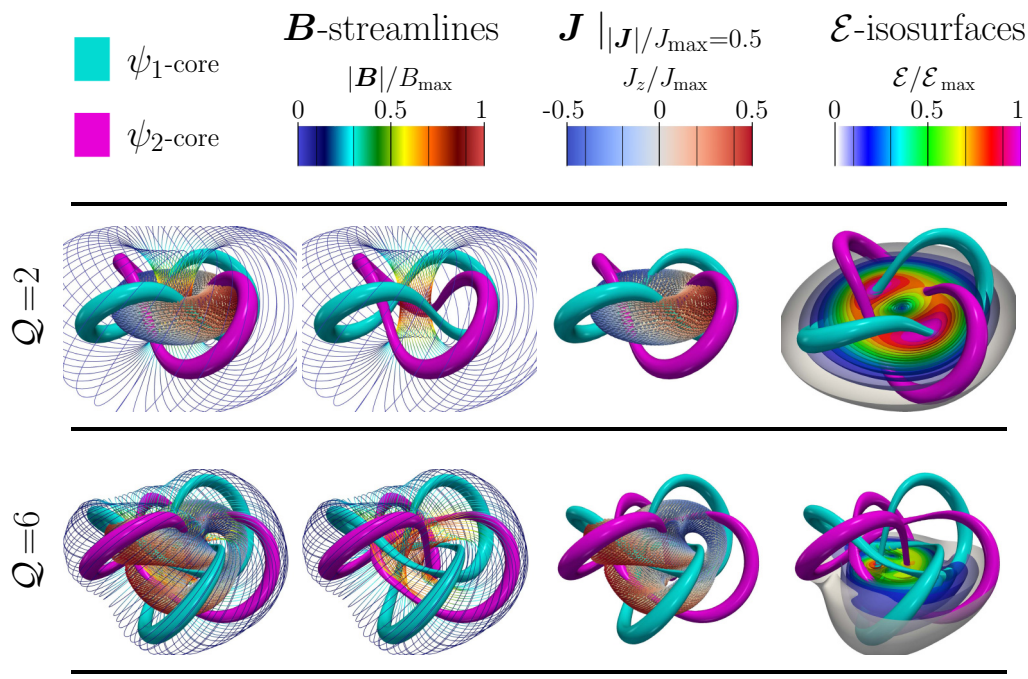


FIG. 1. Detailed structure of two stable vortex knots with different topological charges. Cyan and magenta tubes denote the positions of cores of (fractional) vortices defined as lines for which the densities of component $|\psi_1|^2$ or $|\psi_2|^2$ vanish. Tubes here are density isosurfaces such that $|\psi_{1,2}|^2 = 2.5 \times 10^{-2}$. Panels of the first column show, in addition to vortex cores, a selection of magnetic field streamlines that circulate within the knot (colored according to the magnitude of $|\boldsymbol{B}|$), showing chiral structures of the magnetic field. The second column shows the total current structure $\boldsymbol{J}$ on a selected isosurface where $|\boldsymbol{J}|/J_{\max} = 0.5$. This also shows their chiral structures (colors denote values of the component $J_z$). The last panels show isosurfaces of the energy densities of the vortex knot solutions.

where $\Psi^\dagger\Psi = 1$ (see Appendix A for details). We confirm that typically for superconducting models, vortex knots are unstable. This agrees with the phenomenology of common superconducting materials where, as in superfluids, vortex loops minimize their energy by shrinking. However, we find that properties of knotted vorticity become principally different when Andreev-Bashkin couplings $\hat{\mu}$ are substantially larger than usual gradient couplings $\gamma_a$. Such a disparity between coefficients occurs close to two kinds of critical points. This happens near the phase transition to paired phases caused by strong correlations [37,39,41]. There, the ratio of the stiffnesses of counterflows and coflows of the two components vanishes, implying that the superconductor acquires arbitrarily strong Andreev-Bashkin coupling close enough to the critical point [41]. It can also occur close to the phase transition to Fulde-Ferrel-Larkin-Ovchinnikov (FFLO) state [44,45]. At such transitions, the coefficients $\gamma_a$ change signs (see, e.g., [46,47]), while the Andreev-Bashkin interaction remains nonzero. Two-component FFLO states and corresponding Ginzburg-Landau models were microscopically derived for superconding Dirac metals [47]. Hence, even systems with relatively weak Andreev-Bashkin interactions $\mu_{ab}$ fulfill the above requirements for disparities of coefficients close to a FFLO phase transition. We find that in such regimes, energy minimization from entangled vorticity relaxes to stable vortex knots.

The detailed structure of two obtained stable vortex knots is shown in Fig. 1, for a U(1)×U(1) superconductor, where the parameters $\gamma_a = 0.02$ and $\mu_{ab} = 1$ correspond to a system in the vicinity of the above-mentioned phase transitions. Both topologically different solutions consist of linked and knotted loops of fractional vortices, which are visualized by tubes corresponding to constant-density isosurfaces around their cores. The energy density of knotted solutions is localized close to the knot center, thus emphasizing the particlelike nature of these topological defects (cf. energy density of knotted solitons in the original Skyrme-Faddeev model [18,20,48]). The mechanism responsible for the stability of the solutions follows from the nontrivial scaling of magnetic field energy produced by knotted currents. During the energy minimization process initiated from a large vortex tangle, the solution first shrinks to reduce the kinetic energy of supercurrents. This energy gain is eventually counterbalanced by an increase in magnetic field energy due to the knotted current configuration. By contrast, a topologically trivial vortex loop that does not feature helical or knotted currents (such as a loop of a single fractional vortex) trivially shrinks to zero size.

The superconducting states here support an infinite number of stable solutions corresponding to topologically different ways to tie vortex knots. Figure 2 shows 10 stable knotted vortex loops with the smallest values of the topological index $\mathcal{Q} = 1$–10, in the case of a U(1)×U(1) superconductor. Animations showing the structure of knotted vortices and their formation can be found in the Supplemental Material, movies 1–3 [49]. Solutions with $\mathcal{Q} = 1$–4 consist of two linked fractional vortex loops twisted around one another a varying number of times. For $\mathcal{Q} = 5$ the solution instead is a bound state of two pairs of linked fractional vortex loops. The

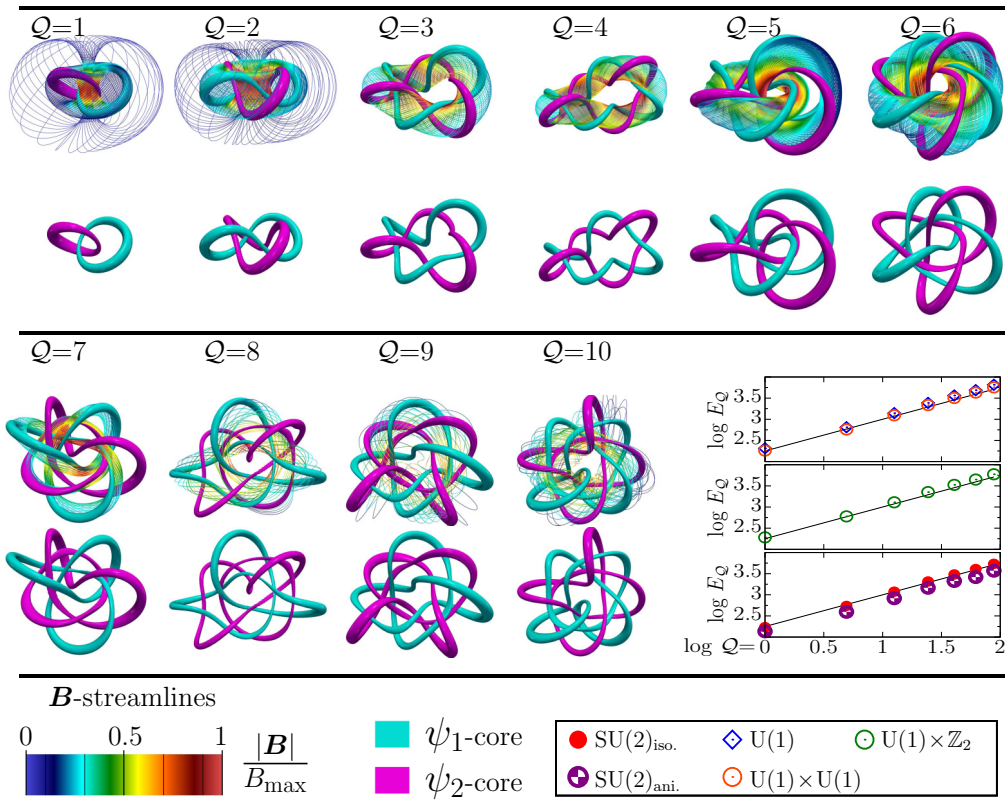


FIG. 2. Solutions for stable knots with topological charges $\mathcal{Q} = 1$–10. Each panel shows obtained numerically stable solutions. They consist of two images: the lower image shows a core structure where as in Fig. 1 cyan and magenta tubes are surfaces enclosing the cores of (fractional) vortices in each component. The upper image shows in addition to vortex cores a selection of magnetic field streamlines circulating within the knot. Note that when increasing the topological index, the structure of the magnetic field streamlines becomes increasingly more complex. The last panel shows the dependence of vortex knot energy $E_\mathcal{Q}$ as a function of the topological index $\mathcal{Q}$. Curves labeled SU(2)$_{\text{iso.}}$, U(1)×$\mathbb{Z}_2$, U(1)×U(1), and U(1) correspond to knotted solutions for different models with various symmetry-breaking potentials while case SU(2)$_{\text{ani.}}$ corresponds to symmetry-breaking gradient terms.

$\mathcal{Q} = 6$ knot consists of two linked trefoil knots. For higher topological indices $\mathcal{Q} = 7$–10 we find that topological structures of the vorticity of different components are inequivalent, thus with solutions forming "isomers.". For example, the $\mathcal{Q} = 7$ knot features a fractional vortex in one component forming a trefoil knot linked to two twisted fractional vortex loops of the other component. For each such isomer solution, there is an energetically degenerate solution where the linked vorticity structure is interchanged between components. We obtained similar stable solutions for two-component models that break SU(2), U(1)×$\mathbb{Z}_2$, and U(1) symmetries. The last panel of Fig. 2 shows that energy of knotted vortices scales with the topological charge as $E_\mathcal{Q} \propto |\mathcal{Q}|^{3/4}$. Remarkably, the power law is the Vakulenko-Kapitansky law of Skyrme-Faddeev model [50]. This scaling of the energy with the topological charge is quite unique, markedly different from the original Skyrme model, where the corresponding exponent is equal to one [51]. This demonstrates that the vortices acquire the properities similar to those of topological excitations in the Skyrme-Faddeev model and therefore the existence of close relationship between the multicomponent gauge theories and the Skyrme-Faddeev model. This implies that vortex knots are not only stable, but when increasing the topological index, knotted vortices minimize their energy by forming complex bound states of knotted and linked fractional vortices.

## V. CONCLUSIONS

The Meissner effect dictates that superconductors can carry magnetic fields and currents only in a thin layer close to their surfaces unless they form quantum vortices. An external magnetic field creates vortex lines that terminate on superconductor surfaces. Field-induced vortices form different collective states (lattices, liquids, and glasses), all featuring distinct transport properties. Closed loops form in the absence of an external field dynamically, e.g., due to quenches or entropically due to thermal fluctuations [6,37]. In ordinary superconductors, vortex loops are not energetically stable and many universal macroscopic properties are dictated by this instability [37]. The instability is a fundamental property of London's hydrodynamics where the smaller is a vortex loop, the smaller are the kinetic energy of supercurrents and magnetic energy. If by contrast the energy associated with a closed vortex loop starts to increase when it shrinks beyond a certain size, a superconductor should exhibit very different basic macroscopic properties. For example, because the production of vortex loops depends on the cooling rate, superfluid stiffness will be history dependent. Slowly cooling through the phase transition or quenching material will produce a different number of loops [52,53] that will not decay, thus differently renormalizing the superfluid stiffness. Moreover,

magnetic properties will also show a history dependence, even in zero-field-cooled setups. Magnetization of ordinary superconductors is determined by the Bean-Livingston barrier [54,55] which the vortices have to overcome to nucleate at a surface. By contrast, if the superconductors described here are rapidly cooled or quenched, they will form stable vortex tangle in their interior. In the case of a sufficiently dense vortex tangle, the barrier for magnetization will have a principally different nature, due to the preexistent vortex tangle.

We showed that under certain conditions, in multicomponent superconductors the properties of vorticity are closer to those in the Skyrme-Faddeev model rather than in the London model. Namely, knotted vorticity becomes stable and acquires conserved Hopf topological invariant.

## ACKNOWLEDGMENTS

We acknowledge discussions with J. Carlström and J. Jäykkä. The computations were performed on resources provided by the Swedish National Infrastructure for Computing (SNIC) at National Supercomputer Center at Linköping, Sweden. The work was supported by the Swedish Research Council Grants No. 642-2013-7837, No. VR2016-06122, and No. VR2018-03659 and Göran Gustafsson Foundation for Research in Natural Sciences and Medicine. This work was performed in part at Aspen Center for Physics, which is supported by National Science Foundation Grant No. PHY-1607611.

## APPENDIX A: NUMERICAL METHODS AND DETAILS OF THE MODEL

The Ginzburg-Landau free-energy features a potential term $U = \nu(\Psi^\dagger\Psi - 1)^2$ responsible for the nonzero superconducting ground state $\Psi^\dagger\Psi \neq 0$. It is supplemented with additional terms that explicitly break the global SU(2) symmetry of $U$ down to different subgroups

$$V[\Psi, \Psi^\dagger] = \sigma|\psi_1|^2|\psi_2|^2 + \eta\left(\psi_1\psi_2^* + \psi_1^*\psi_2\right). \tag{A1}$$

Solutions were obtained for parameters of kinetic term $\gamma_a = 0.02$ and of current coupling coefficients $\mu_{ab} = 1$ for $a, b = 1, 2$ [except of the $\mathrm{SU}(2)_{\mathrm{ani.}}$ case described below]. To demonstrate that the existence of stable knotted vortices does not rely on a specific symmetry of the model, we performed computations with various representative symmetry-breaking potentials: (i) U(1): $\sigma = -10^{-4}$, $\eta = -5 \times 10^{-5}$; (ii) $\mathrm{U}(1)\times\mathbb{Z}_2$: $\sigma = 10^{-4}$, $\eta = 0$; (iii) $\mathrm{U}(1)\times\mathrm{U}(1)$: $\sigma = -10^{-4}$, $\eta = 0$; (iv) SU(2), iso.: $\sigma = 0$, $\eta = 0$; SU(2), ani.: for this particular case the ground state is invariant under SU(2) rotations, but current-current coupling coefficients were chosen to break this symmetry: $\mu_{11} = \mu_{22} = 0.97$ and $\mu_{12} = \mu_{21} = 1$. Symmetry-breaking parameters were chosen to be small to prevent important changes in intrinsic length scales and thus to prevent substantial changes in the solution size relative to the numerical lattice spacing. This allowed us to make quantitatively accurate comparisons of knotted solutions for different symmetry-breaking potentials. Note that in all cases the functional is positively defined. In the special case (iv) the functional is positively defined only in the London limit, i.e., as long as the total density is fixed to unity.

In our preliminary simulations, we considered various values of coefficient $\nu$. When stable vortex knots exit they have no zeros of total density. The stability properties of solutions typically improve with increasing $\nu$. However, such a regime significantly inhibits the convergence of conventional methods of minimization. This phenomenon is directly related to well-known disadvantages of the penalty function method. Thus, after finding stable solutions, with different indices $\mathcal{Q}$ in several simulations with variable total density, and observing no core crossing of the cores of fractional vortices in different components in these configurations, we reduced the size of the parameter space by focusing on the London limit where $\Psi^\dagger\Psi = 1$ to systematically investigate solutions with a topological index of $\mathcal{Q} = 1$ to $\mathcal{Q} = 10$.

For a computationally efficient investigation of the London limit, we used the "Atlas" method, which is based on the efficient navigation of coordinate charts for the order-parameter manifold, which here is an $\mathbb{S}^3_\Psi$ (for further information on the method, see the Supplemental Materials section given in Ref. [56]). This is advantageous in that this automatically satisfies the constraint in contrast to the conventional minimization techniques.

Fields were discretized using a second-order accuracy finite-difference scheme and a homogeneous cuboidal mesh with a lattice spacing of 0.5. The grid used consisted of $160^3$ nodes for solutions with $Q \leqslant 7$ and $224^3$ nodes for higher topological charges. To ensure that the solutions were not artifacts of a finite-simulation domain, we considered both "fixed" and "free" boundary conditions. Energy was minimized by applying a nonlinear conjugate gradient (NCG) method and the Polak-Ribière-Polyak formula. We used a branched approach to standard NCG by separating all degrees of freedom into two sets: one associated with gauge degrees of freedom $\mathbf{A}$ and another with superconducting degrees of freedom $\psi_a$. Accordingly, the conventional linear search routine of the NCG method was replaced with a two-dimensional search. By separating numerical degrees of freedom according to their physical features, this approach significantly accelerates the convergence speed of the algorithm. The termination criterion for convergence was chosen according to [57] with a function tolerance $\tau_F = 10^{-10}$. The algorithm was parallelized for NVIDIA CUDA-enabled graphics processor units. Calculations were performed on a set of two video cards with microprocessors GP102-350-K1-A1. To achieve optimal performance, most computations were realized using a single-precision floating-point format (32 bits). To offset truncation errors from the single-precision arithmetic, we used the Kahan summation algorithm [58] and a parallel reduction technique suitable for CUDA [59].

To cross validate our results, we performed simulations extending beyond the London limit using a different approach based on finite-element methods and found consistent results. Fields were discretized within a framework provided by the FreeFem++ library [60]. Most of the simulations were performed on four two-socket nodes with 8-core Intel Xeon E5-2660 processors.

## APPENDIX B: CALCULATION OF A TOPOLOGICAL INDEX OF VORTEX KNOTS

Different vortex knots are characterized by an integer index/invariant $\mathcal{Q}$ associated with the topological properties of the maps $\mathbb{S}^3 \to \mathbb{S}^3_\Psi$. To calculate this invariant, the superconducting order-parameter field $\Psi$ is cast into a four-dimensional vector $\zeta = (\mathrm{Re}\,\psi_1, \mathrm{Im}\,\psi_1, \mathrm{Re}\,\psi_2, \mathrm{Im}\,\psi_2)/\sqrt{\Psi^\dagger\Psi}$. Note that for $\zeta$ to be well defined, there should be no zeros of $\Psi$, i.e., no overlap between core centers of fractional vortices in both components. When cores of fractional vortices in different components can cross one another, this generates a point where $\Psi^\dagger\Psi = 0$, then the topological index $\mathcal{Q}$ is not an invariant. Namely, it can discretely change from different integer values when fractional vortices in different components cross one another. Note that when knots are unstable, the invariant changes when they collapse to a size comparable with that of the numerical lattice. In the regime where knots are stable, the crossing of the fractional vortex cores is prevented by a barrier associated with magnetic energy. This leads to the emergence of the following topological invariant.

The finiteness of energy implies that a superconductor should be in the ground state at spatial infinity. It follows that infinity is identified with a single field configuration (up to gauge transformations). Hence, the vector field $\zeta(\mathbf{r})$ is a map from the one-point compactified space to the target 3-sphere $\zeta : \mathbb{S}^3 [\cong \mathbb{R}^3 \cup \{\infty\}] \to \mathbb{S}^3_\Psi$. Maps between 3-spheres fall into disjoint homopoty classes, the elements of the third homotopy group $\pi_3(\mathbb{S}^3_\Psi)$, which is isomorphic to integers: $\pi_3(\mathbb{S}^3_\Psi) = \mathbb{Z}$. Thereby, $\zeta$ is associated with an integer number, the degree of the map $\zeta$ is $\deg\zeta$, which counts how many times the target sphere $\mathbb{S}^3_\Psi$ is wrapped while covering the whole $\mathbb{R}^3$ space. Field configurations are thus characterized by the topological index $\mathcal{Q} := \deg\zeta$ which is calculated using Eq. (3). As discussed, for example, in [23], the degree of $\zeta$, $\mathcal{Q}$ is equal to the Hopf charge of the combined Hopf map $h \circ \zeta : \mathbb{S}^3 \to \mathbb{S}^2$. Formula (3) was used to calculate the topological invariant of numerically obtained stable knotted vortex configurations. It was numerically found to be an integer with an accuracy level ranging within a few percent.

## APPENDIX C: INITIAL STATES USED FOR ENERGY-MINIMIZATION CALCULATIONS

The energy-minimization calculations were performed for a variety of vorticity-generating initial states. The initial states included (i) textures based on hedgehog-type ansatz, (ii) closely spaced pairs of such a textures, (iii) linked vortex loops, and (iv) textures based on rational map ansatz. All of the initial guesses were giving consistent results.

One of the easiest-to-construct initial cases that we extensively used was based on a hedgehog-type texture [61]

$$(\zeta_1', \zeta_2', \zeta_3') = \mathbf{m}\sin(\chi), \quad \zeta_4' = \cos(\chi), \tag{C1}$$

where the unit vector field $\mathbf{m}$ is defined as

$$m_1 + im_2 = \sin(\vartheta)e^{-iQ\phi}, \quad m_3 = \cos(\vartheta),$$

and the shape function

$$\chi = \pi(1 + (r/r_0)^2 e^{(r/r_0)^2})^{-1},$$

where $r$, $\vartheta$, $\phi$ are the spherical coordinates, and $r_0$ is a tunable parameter that sets the appropriate scale of the texture. For the initial state to satisfy appropriate behavior at $r \to \infty$, the vector $\zeta'$ must be rotated: $\zeta = R \cdot \zeta'$. The generic rotation matrix and a particular one $\tilde{R}$ in the case of the potential yielding a $\mathrm{U}(1)\times\mathbb{Z}_2$ symmetry of the ground state are defined as follows:

$$R = \frac{1}{2}\begin{pmatrix} 1 & 1 & -1 & 1 \\ -1 & 1 & 1 & 1 \\ 1 & -1 & 1 & 1 \\ -1 & -1 & -1 & 1 \end{pmatrix},$$

$$\tilde{R} = \frac{1}{\sqrt{2}}\begin{pmatrix} 0 & 0 & -1 & 1 \\ 0 & 0 & 1 & 1 \\ 1 & -1 & 0 & 0 \\ -1 & -1 & 0 & 0 \end{pmatrix}. \tag{C2}$$

Thus, at the boundaries of the simulation domain superconducting degrees of freedom assume $\zeta = (1, 1, 1, 1)/2$, except in the case of $\mathrm{U}(1)\times\mathbb{Z}_2$ symmetry where $\zeta = (1, 1, 0, 0)/\sqrt{2}$. The vector potential is initially set as a pure gauge $\mathbf{A} = 0$.

This initial state generates linked vorticity for which the topological charge $Q$ is an input parameter. We found that for the regimes with stable knots, the total topological charge remains invariant throughout minimization. In the Supplemental Material, video 4 [49] demonstrates the minimization process, starting from the initial state (C1) with $Q = 2$. This and all of the Supplemental Material movies [49] described below were recorded for the case $\sigma = -10^{-4}$, $\eta = 0$. To obtain solutions with a high topological index $\mathcal{Q}$, we placed two separated textures along the main diagonal of the computational domain with charges of $\mathcal{Q}_{1,2}$ such that $\mathcal{Q}_1 + \mathcal{Q}_2 = \mathcal{Q}$. For example, to construct a $\mathcal{Q} = 1$ solution, the starting configuration was set to $\mathcal{Q}_1 = -1$, $\mathcal{Q}_2 = 2$; for $\mathcal{Q} = 2$, we used $\mathcal{Q}_1 = \mathcal{Q}_2 = 1$, etc. During minimization, the two initially separated textures were attracted to one another and eventually merged into a single texture. The approach of starting with two well-separated vorticity-seeding initial states, rather than a single one, is very efficient. This is because it breaks spatial symmetries, thus minimizing the chance of being trapped in long-living unstable or weakly metastable states. The Supplemental Material video 5 [49] demonstrates the minimization process, starting from two closely spaced textures with $\mathcal{Q}_1 = \mathcal{Q}_2 = 1$.

The Supplemental Material video 6 [49] demonstrates the minimization process, starting with three circular vortex loops having two links. Similarly to the cases presented in Supplementary Material movies 4 and 5 [49] this leads to the same solution with $Q = 2$.

The Supplemental Material video 7 [49] demonstrates the minimization process with the initial state corresponding to rational map ansatz for baryon number $|B| = 3$ in "tetrahedral" case [62]. Such an initial condition, as well as an axially symmetric ansatz (C1) with $Q = 3$ (see Supplemental Material video 8 [49]), lead to the same solution.

[1] W. Thomson (Lord Kelvin), On Vortex Atoms, Proceedings of the Royal Society of Edinburgh **VI**, 94 (1867) [Reprinted in Philos. Mag. **XXXIV**, 1867, pp. 15-24].

[2] P. G. Tait, *On Knots I II, and III*, Scientific Papers (Cambridge University Press, Cambridge, 1898), Vol. 1, pp. 273–347.

[3] T. H. R. Skyrme, A unified field theory of mesons and baryons, Nucl. Phys. **31**, 556 (1962).

[4] L. Onsager, Statistical hydrodynamics, Il Nuovo Cimento **6**, 279 (1949).

[5] R. P. Feynman, Application of quantum mechanics to liquid helium, Prog. Low Temp. Phys. **1**, 17 (1955).

[6] C. Dasgupta and B. I. Halperin, Phase Transition in a Lattice Model of Superconductivity, Phys. Rev. Lett. **47**, 1556 (1981).

[7] J. M. Kosterlitz and D. J. Thouless, Long range order and metastability in two dimensional solids and superfluids. (Application of dislocation theory), J. Phys. C: Solid State Phys. **5**, L124 (1972).

[8] V. L. Berezinskiĭ, Destruction of long-range order in one-dimensional and two-dimensional systems having a continuous symmetry group I. Classical Systems, Zh. Eksp. Teor. Fiz. **59**, 907 (1970) [Sov. Phys.-JETP **32**, 493 (1971)].

[9] G. H. Derrick, Comments on nonlinear wave equations as models for elementary particles, J. Math. Phys. **5**, 1252 (1964).

[10] R. A. Battye, N. R. Cooper, and P. M. Sutcliffe, Stable Skyrmions in Two-Component Bose-Einstein Condensates, Phys. Rev. Lett. **88**, 080401 (2002).

[11] E. Radu and M. S. Volkov, Existence of stationary, non-radiating ring solitons in field theory: knots and vortons, Phys. Rep. **468**, 101 (2008).

[12] W. T. M. Irvine and D. Bouwmeester, Linked and knotted beams of light, Nat. Phys. **4**, 716 (2008).

[13] P. Sutcliffe, Skyrmion Knots in Frustrated Magnets, Phys. Rev. Lett. **118**, 247203 (2017).

[14] D. Kleckner and W. T. M. Irvine, Creation and dynamics of knotted vortices, Nat. Phys. **9**, 253 (2013).

[15] W. Lee, A. H. Gheorghe, K. Tiurev, T. Ollikainen, M. Möttönen, and D. S. Hall, Synthetic electromagnetic knot in a three-dimensional skyrmion, Sci. Adv. **4**, eaao3820 (2018).

[16] L. D. Faddeev, Quantization of Solitons, in Report No. IAS Print-75-QS70, Institute for Advanced Study, Princeton, NJ, 1975 (unpublished).

[17] J. Gladikowski and M. Hellmund, Static solitons with non-zero Hopf number, Phys. Rev. D **56**, 5194 (1997).

[18] L. D. Faddeev and A. J. Niemi, Knots and particles, Nature (London) **387**, 58 (1997).

[19] R. A. Battye and P. M. Sutcliffe, Knots as Stable Soliton Solutions in a Three-Dimensional Classical Field Theory, Phys. Rev. Lett. **81**, 4798 (1998).

[20] J. Hietarinta and P. Salo, Faddeev-Hopf knots: Dynamics of linked un-knots, Phys. Lett. B **451**, 60 (1999).

[21] E. Babaev, L. D. Faddeev, and A. J. Niemi, Hidden symmetry and knot solitons in a charged two-condensate Bose system, Phys. Rev. B **65**, 100512(R) (2002).

[22] E. Babaev, Dual Neutral Variables and Knot Solitons in Triplet Superconductors, Phys. Rev. Lett. **88**, 177002 (2002).

[23] J. Jäykkä, J. Hietarinta, and P. Salo, Topologically nontrivial configurations associated with Hopf charges investigated in the two-component Ginzburg-Landau model, Phys. Rev. B **77**, 094509 (2008).

[24] E. Babaev, Non-Meissner electrodynamics and knotted solitons in two- component superconductors, Phys. Rev. B **79**, 104506 (2009).

[25] J. Jäykkä and J. M. Speight, Supercurrent coupling destabilizes knot solitons, Phys. Rev. D **84**, 125035 (2011).

[26] A. Gorsky, M. Shifman, and A. Yung, Revisiting the Faddeev-Skyrme model and Hopf solitons, Phys. Rev. D **88**, 045026 (2013).

[27] R. S. Ward, Stabilizing textures with magnetic fields, Phys. Rev. D **66**, 041701(R) (2002).

[28] A. Samoilenka and Ya. Shnir, Fractional Hopfions in the Faddeev-Skyrme model with a symmetry breaking potential, J. High Energy Phys. 09 (2017) 029.

[29] Y. Wang, G. Y. Cho, T. L. Hughes, and E. Fradkin, Topological superconducting phases from inversion symmetry breaking order in spin-orbit-coupled systems, Phys. Rev. B **93**, 134512 (2016).

[30] Y. Wang and L. Fu, Topological Phase Transitions in Multicomponent Superconductors, Phys. Rev. Lett. **119**, 187003 (2017).

[31] O. Sjöberg, On the Landau effective mass in asymmetric nuclear matter, Nucl. Phys. A **265**, 511 (1976).

[32] N. Chamel, Two-fluid models of superfluid neutron star cores, Mon. Not. R. Astron. Soc. **388**, 737 (2008).

[33] E. Babaev, A. Sudbø, and N. W. Ashcroft, A superconductor to superfluid phase transition in liquid metallic hydrogen, Nature (London) **431**, 666 (2004).

[34] E. Babaev and N. W. Ashcroft, Violation of the London law and Onsager-Feynman quantization in multicomponent superconductors, Nat. Phys. **3**, 530 (2007).

[35] P. B. Jones, Type I and two-gap superconductivity in neutron star magnetism, Mon. Not. R. Astron. Soc. **371**, 1327 (2006).

[36] A. F. Andreev and E. P. Bashkin, Three-velocity hydrodynamics of superfluid solutions, Zh. Eksp. Teor. Fiz. **69**, 319 (1975) [Sov. Phys.-JETP **42**, 164 (1975)].

[37] B. V. Svistunov, E. S. Babaev, and N. V. Prokof'ev, *Superfluid States of Matter* (Taylor & Francis, London, 2015).

[38] A. J. Leggett, A theoretical description of the new phases of liquid $^3$He, Rev. Mod. Phys. **47**, 331 (1975).

[39] A. B. Kuklov and B. V. Svistunov, Counterflow Superfluidity of Two-Species Ultracold Atoms in a Commensurate Optical Lattice, Phys. Rev. Lett. **90**, 100401 (2003).

[40] Ş. G. Söyler, B. Capogrosso-Sansone, N. V. Prokof'ev, and B. V. Svistunov, Sign-alternating interaction mediated by strongly correlated lattice bosons, New J. Phys. **11**, 073036 (2009).

[41] K. Sellin and E. Babaev, Superfluid drag in the two-component Bose-Hubbard model, Phys. Rev. B **97**, 094517 (2018).

[42] J. Garaud, K. A. H. Sellin, J. Jäykkä, and E. Babaev, Skyrmions induced by dissipationless drag in U(1) × U(1) superconductors, Phys. Rev. B **89**, 104508 (2014).

[43] E. Babaev, Vortices with Fractional Flux in Two-Gap Superconductors and in Extended Faddeev Model, Phys. Rev. Lett. **89**, 067001 (2002).

[44] A. I. Larkin and Y. N. Ovchinnikov, Inhomogeneous state of superconductors(production of superconducting state in ferromagnet with Fermi surfaces, examining Green function), Zh. Eksp. Teor. Fiz. **47**, 1136 (1964) [Sov. Phys.-JETP **20**, 762 (1965)].

[45] P. Fulde and R. A Ferrell, Superconductivity in a strong spin-exchange field, Phys. Rev. **135**, A550 (1964).

[46] A.I. Buzdin and H. Kachkachi, Generalized Ginzburg-Landau theory for nonuniform FFLO superconductors, Phys. Lett. A **225**, 341 (1997).

[47] M. Barkman, A. A. Zyuzin, and E. Babaev, Antichiral and nematicity-wave superconductivity, Phys. Rev. B **99**, 220508 (2019).

[48] P. Sutcliffe, Knots in the Skyrme–Faddeev model, Proc. R. Soc. London A **463**, 3001 (2007).

[49] See Supplemental Material at http://link.aps.org/supplemental/10.1103/PhysRevB.100.094515 for movies showing the structure of knotted vortices and the process of energy minimization.

[50] A. F. Vakulenko and L. V. Kapitanskii, Stability of solitons in $S^2$ in the nonlinear $\sigma$-model, Dokl. Akad. Nauk USSR **246**, 840 (1979) [Sov. Phys. Dokl. **24**, 433 (1979)].

[51] L. D. Faddeev, Some comments on the many-dimensional solitons, Lett. Math. Phys. **1**, 289 (1976).

[52] T. W. B. Kibble, Topology of cosmic domains and strings, J. Phys. A: Math. Gen. **9**, 1387 (1976).

[53] W. H. Zurek, Cosmological experiments in superfluid helium? Nature (London) **317**, 505 (1985).

[54] C. P. Bean and J. D. Livingston, Surface Barrier in Type-II Superconductors, Phys. Rev. Lett. **12**, 14 (1964).

[55] P. G. De Gennes, Vortex nucleation in type ii superconductors, Solid State Commun. **3**, 127 (1965).

[56] F. N. Rybakov, A. B. Borisov, S. Blügel, and N. S. Kiselev, New Type of Stable Particlelike States in Chiral Magnets, Phys. Rev. Lett. **115**, 117201 (2015).

[57] P. E. Gill, W. Murray, and M. H. Wright, *Practical Optimization* (Academic, New York, 1981).

[58] W. Kahan, Pracniques: Further Remarks on Reducing Truncation Errors, Commun. ACM **8**, 40 (1965).

[59] J. Luitjens, Faster Parallel Reductions on Kepler, NVIDIA Documentation, 2014 (unpublished).

[60] F. Hecht, New development in freefem++, J. Numer. Math. **20**, 251 (2012).

[61] T. H. R. Skyrme, A non-linear field theory, Proc. R. Soc. London Sect. A **260**, 127 (1961).

[62] C. J. Houghton, N. S. Manton, and P. M. Sutcliffe, Rational maps, monopoles and Skyrmions, Nucl. Phys. B **510**, 507 (1998).